Proceedings of Ninth World Conference on Earthquake Engineering
August 2-9, 1988, Tokyo-Kyoto, JAPAN (Vol.VI)

10-5-5

AN EVALUATION METHOD FOR RESTORING FORCE CHARACTERISTICS OF R/C SHEAR WALLS OF REACTOR BUILDINGS

H. TANAKA[1] K. IMOTO[2] S. YOSHIZAKI[3] K. EMORI[4] Y. INADA[5] H. NANBA[6]

[1] The Tokyo Electric Power Services Co., Ltd. [2] Ohbayashi Corporation
[3] Taisei Corporation [4] Kajima Corporation
[5] Shimizu Corporation [6] Takenaka Corporation

SUMMARY

In the nonlinear dynamic response analysis of reactor buildings, restoring force characteristics must be provided, which can precisely predict the nonlinear behavior of shear walls up to the ultimate strength. This paper describes an investigation to establish a standard evaluation method by the extensive and rigorous reviews of the existing experimental results.

INTRODUCTION

In the seismic design for reactor buildings, nonlinear dynamic response analysis plays an important role in both examining the seismic safety of buildings and evaluating the response of related equipment. In recent years, a number of model tests have been carried out for reinforced concrete (R/C) shear walls in reactor buildings, which provide a large stock of test data with many new findings on restoring force characteristics. This paper proposes an evaluation method for restoring force characteristics of R/C shear walls based on the reviews of these existing test data in Japan. It provides a standard evaluation method for restoring force characteristics to be used for nonlinear dynamic response analyses of reactor buildings. In the analyses shear deformations and bending deformations of a wall are treated independently. The restoring force characteristics are assigned in terms of shear stress-strain relationship (referred to as τ-γ relationship hereafter) and of bending moment-curvature relationship (referred to as M-ϕ relationship hereafter), respectively. This paper proposes skeleton curves with practical hysteresis models modified so as to closely resemble the test results.

OUTLINE OF THE SPECIMENS REFERENCED

The scope of the survey is restricted to the horizontal loading tests conducted on shear walls that constitute principal earthquake resistant components of reactor buildings. The configuration of the specimens investigated comprise 22 box walls, 26 R/C cylindrical walls, 19 cylindrical walls under prestressed force and/or internal pressure, 3 truncated conical walls, 9 octagonal tube walls and 24 I-shaped section walls, which amount to 103 specimens. As for dimensions of the specimens, the center-to-center distances between tensile and compression flanges (D) were typically found between 100 and 200cm, while the wall thicknesses (t) were between 5 and 10cm. This corresponded to 1/10 to 1/30 scale of actual dimension of shear walls in reactor buildings. The shear span ratios (M/QD) were distributed between 0.5 and 1.5. The compressive strength of concrete of the specimens was normally found between 240kg/cm^2 and 260kg/cm^2. While several specimens exclusively designed for Prestressed Concrete Containment Vessel (PCCV) showed a compressive strength greater than 400kg/cm^2. The reinforcement ratios agreed considerably with those of real reactor buildings. Most of the ratios were lower than 1.2%. Of the 103 specimens, 67 were useful for discussion on the skeleton curves, 48 were for discussion on the hysteresis rules and 23 were only useful for discussion on the ultimate loads.

SKELETON CURVE FOR τ-γ RELATIONSHIP

Skeleton Curve The skeleton curve for τ-γ relationship is idealized as a tri-linear curve with three control points (τ_1, γ_1), (τ_2, γ_2) and (τ_3, γ_3) respectively, as shown in Fig. 1. These control points can be defined as follows;

1st point

$$\tau_1 = \sqrt{\sqrt{Fc}\ (\sqrt{Fc} + \sigma v\ )} \qquad (1)$$

$$\gamma_1 = \tau_1\ /G \qquad (2)$$

2nd point

$$\tau_2 = 1.35\tau_1 \qquad (3)$$

$$\gamma_2 = 3\gamma_1 \qquad (4)$$

ultimate point

$$\tau_3 = \{1 - \tau s/\ (4.5\sqrt{Fc}\ )\}\ \tau_0 + \tau_s \quad ;\ \text{for } \tau_s \leqq 4.5\sqrt{Fc} \qquad (5\text{-}1)$$

$$= 4.5\sqrt{Fc} \quad ;\ \text{for } \tau_s > 4.5\sqrt{Fc} \qquad (5\text{-}2)$$

$$\gamma_3 = 4.0 \times 10^{-3} \qquad (6)$$

where,

$$\tau_0 = (3 - 1.8M\ /\ QD)\sqrt{Fc} \qquad (M/QD = 1\ ;\ \text{if } M/QD > 1)$$

$$\tau_s = (P_V + P_H)\ {}_s\sigma_y/2 + (\sigma V + \sigma H)/2$$

Fc : compressive strength of concrete (kg/cm^2)

G : shear modulus of concrete (kg/cm^2)

cE : Young's modulus of concrete (kg/cm^2)

P_V, P_H : reinforcement ratio in vertical and horizontal direction, respectively

σ_V,σ_H : axial stress in vertical and horizontal direction, respectively (kg/cm^2)

${}_s\sigma_y$: yielding stress of a reinforcing bar (kg/cm^2)

M/QD : shear span ratio

Verification The equation (1) corresponds to the average shear stress at the initiation of central oblique cracking in the walls subjected to in-plane shear forces (Ref.1). As seen in Table 1 and Fig. 3(a), the average of the ratios of the experimental values to the theoretical values is 0.98, indicating that the model approximation is satisfactory. The equation (2) for determining the shear strain corresponding to τ_1 uses the elastic stiffness in the $\tau-\gamma$ relationship with the shear modulus G. The experimental results for the $\tau-\gamma$ relationship indicate that the stiffness after cracking takes a shape of convex curve. To obtain the approximate curve for this empirical curve, γ_2=3γ_1 is assumed and the corresponding τ is examined from these curves. Then the ratio of τ_2 to the corresponding value τ_1, or β is obtained for each test and shown in Fig. 3(b).The average value of β, 1.35, gives good approximation to the experimental results.

For the ultimate shear stress, the equation (5) which is derived by taking the stress carried by the reinforcing bars as well as the stress carried by the concrete into account (Ref.2). As shown in Table 1 and Fig. 3 (c), the average of the ratios between the experimental values and the corresponding calculated values is 1.04, evidencing that the proposed equation approximates the behaviors of actual walls fairly well, although a slight fluctuation of the ratios could be observed. Moreover, the experimental values for the I-shaped section walls having a large amount of vertical reinforcement in flange walls are excluded as these walls are not found in any real reactor building, the average value of β and that of the standard deviation may be further improved. Around the ultimate strength level, the experimental $\tau-\gamma$ relationships of the cylindrical walls or octagonal tube walls have relatively large deformation capacity as compared with the box walls or I-shaped section walls. Considering the fact that the difference of the ultimate shear strain among shear walls of different configuration is yet to be investigated and that the experimental values of the ultimate shear strain fluctuate considerably, the ultimate shear strain is set uniquely to 4×10^{-3}(Ref.3).

SKELETON CURVE FOR M-Φ RELATIONSHIP

Skeleton Curve The skeleton curve for M-φ relationship is idealized as a tri-linear curve with three control points (M_1, ϕ_1), (M_2, ϕ_2) and (M_3, ϕ_3) respectively, as shown in Fig. 2. These control points can be defined as follows;

1st point
$$M_1 = Ze\ (ft + \sigma v) \tag{7}$$
$$\varnothing_1 = M_1/(cE \cdot Ie) \tag{8}$$

2nd point
$$M_2 = My \tag{9}$$
$$\varnothing_2 = \varnothing y \tag{10}$$

ultimate point
$$M_3 = Mu \tag{11}$$
$$\varnothing_3 = 0.004/Xnu \quad (\varnothing_3 = 20\varnothing_2\ ;\ \text{if}\ \varnothing_3 > 20\varnothing_2) \tag{12}$$

where,

Ie : moment of inertia of a cross section including reinforcement (cm^4)
Ze : section modulus including reinforcement (cm^3)
ft : tensile strength of concrete (kg/cm^2) ; $ft = 1.2\ \sqrt{Fc}$
My : bending moment when tensile reinforcement reaches the yielding state (kg·cm)
Φy : curvature of walls when tensile reinforcement reaches the yielding state (1/cm)
D : center-to-center distance between tensile and compression flanges (cm)
Mu : full plastic moment (kg·cm)
Xnu : distance from extreme compression fiber to neutral axis at full plastic stage(cm)

Verification For verification of the proposed model, the experimental values of the bending moment (M) and the bending rotation (R_B) in the base of test specimens are used. Additional deformations due to an elongation and a slip of the tensile reinforcing bars in the base are considered as rotation [4]. The M-R_B relationship for the experiment is also expressed with a tri-linear curve. The equation (7) for determining the bending moment for the first point is obtained by summing the fiber stress at the initiation of flexural cracking, $1.2\ \sqrt{Fc}$, and the axial stress. Fig. 5(a) shows a comparison of the loads at the initiation of flexural cracking in the experiments and the calculations. Fig. 5(b) shows the experimental results of the bending moment at the first point and the calculated results in comparison. The averages of the ratios between the experimental results and the calculated results (referred to as R_E/c hereafter) are 0.87 and 1.10, respectively. These figures indicate that the calculated values for the load at the initiation of flexural cracking are slightly higher than the experimental values, while those of the bending moment at the first point in the M-R_B relationship are a little lower than the actual experimental results. The equation (8) for determining the curvature at the first point is derived by defining the initial stiffness of the M-φ relationship skeleton curve as the product of Young's modulus of concrete (cE) and the moment of inertia of cross section (Ie), cE·Ie.

The equations (9) and (10) for determining the bending moment (M_2) and the curvature (ϕ_2) for the second point are defined respectively as the moment and the curvature when the tensile reinforcement reaches the yielding state based on the Bernoulli-Eulerian theory. As seen in Fig. 5(c), the average of R_E/c is 1.07, shown that the calculated results generally agree with the experimental results. As seen in Fig. 5(d), the average of R_E/c for the ultimate point is 1.44, indicating that the experimental results considerably surpass the calculated results.

The ultimate bending moment (M_3) is defined as the full plastic moment at flexural failure of the compression side of concrete. The stress of the compression side of concrete and that of the tension side of reinforcement at this moment is set to be 0.85 Fc and ${}_s\sigma_y$, respectively. The equation (12) for determining the ultimate curvature (ϕ_3) is obtained by assuming the strain of extreme compression fiber as 0.004. In case of walls with small axial stress and reinforcement ratio, the neutral axis possibly moves into the compression zone of flange walls, making the ultimate curvature extremely large. However, such phenomena will not be found in real reactor buildings. Therefore, the upper limit of ϕ_3 is set to be 20 ϕ_2.

HYSTERESIS MODELS

The hysteresis models adopted here for the τ-γ, and the M-ϕ relationships include the following characteristics, respectively. These models are determined so as to be practical enough to be used for a dynamic response analysis.

τ-γ Relationship (Fig.5)

(1) The hysteresis model for the τ-γ relationship is set to be a peak-to-peak oriented system.

(2) A stable loop does not have any area corresponding to the hysteretic energy loss.

(3) The unloading path from the maximum (or minimum) value point beyond the first control point draws a straight line that connects the maximum (or minimum) value point with the minimum (or maximum) value point on the opposite side. If the minimum (or maximum) value point on the opposite side does not exceed the first control point on the skeleton curve, the first control point is regarded as the minimum (or maximum) value point.

M-ϕ Relationship (Fig.6)

(1) The hysteresis model for the M-ϕ relationship is also set to be a peak-to-peak oriented system.

(2) A stable loop dose not have any area corresponding to the hysteretic energy loss up to the second control point.

(3) The unloading path from the maximum (or minimum) value point beyond the second control point forms a stable loop in such a way that the path is directed towards the peak ever reached on the oppositeside. If the minimum (or maximum) value point on the opposite side does not exceed the second control point on the skeleton curve, the second control point is assumed as the minimum (or maximum) value point.

(4) The skeleton curve is of a degrading-trilinear type whose stable loop forms a parallelogram so long as the maximum value point exceeds the second control point. The area of hysteresis loop varies in accordance with an equivalent viscous damping in proportion to the maximum curvature. The lower corner point of the parallelogram is defined as a point where the moment is smaller than that of the maximum value point by Ms, as shown in Fig.6 (c).

CONCLUSION

A standard evaluation method for restoring force characteristics required in nonlinear dynamic response analysis of nuclear plant reactor buildings is proposed based on the extensive reviews of the existing test data on R/C shear walls in reactor buildings in Japan. Reliability of the equations to specify each control point on the skeleton curves has been examined by comparing the ratio of calculated values and the averaged experimental ones and by analyzing the standard deviations of the test results. The present study will provide the basic data for statistical treatment of the behavior of reactor buildings during a very severe earthquake.

ACKNOWLEDGMENTS

This research is a summary of investigations for the "Evaluation Method of the Safety Margins of Reactor Buildings to Earthquake Ground Motion", sponsored by the ten electric power companies in Japan.

REFERENCES

1. Inada, Y., "Restoring Force Characteristics of Reactor Buildings Based on Load Tests and Numerical Analysis" Transactions of A.I.J. No. 371 Jan., 1987
2. Yoshizaki, S. et al., "Shear Strength of Shear Walls with Numerous Small Openings" 5th Annual Research Presentation Meeting on Concrete Engineering, 1983
3. Tomii, M., "Note on Ultimate Strength Design of R/C Structures No.31" J. of Architecture and Building Science, AIJ July, 1982
4. Otani, S., "Inelastic Analysis of R/C Frame Structures" J. of Structural Division, ASCE July, 1974

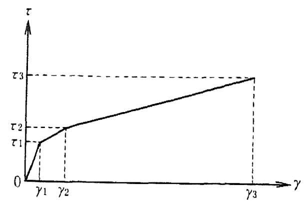

Fig. 1 Skeleton Curve for $\tau-\gamma$ Relationship

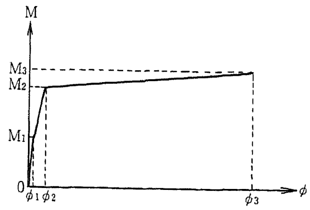

Fig. 2 Skeleton Curve for $M-\phi$ Relationship

Specimen configuration	Axial force	
	without	with
box wall	□	■
box wall subjected to diagonal load	◇	
cylindrical wall	○	●
truncated conical wall	△	▲
hexagonal tube wall	⬡	
thick hexagonal tube wall	⬡ (double)	
I-shaped section wall	⊢⊣	⊢⊣ (filled)

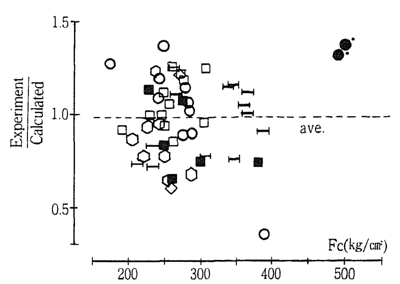

(a) Comparison of τ_1 Values at lst Point

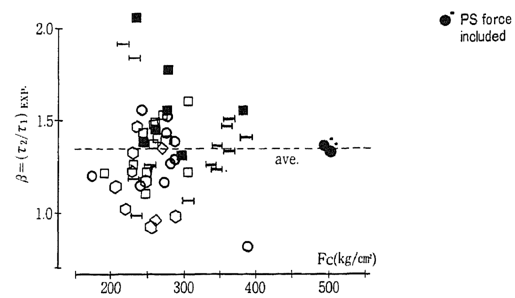

(b) Distribution of β Values Obtained from Test Data.

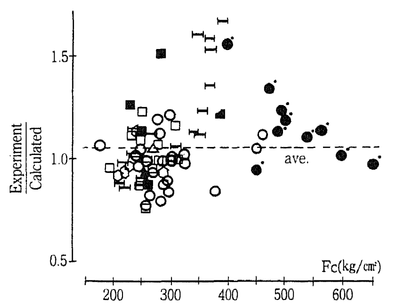

(c) Comparison of τ_3 Values at Ultimate Point

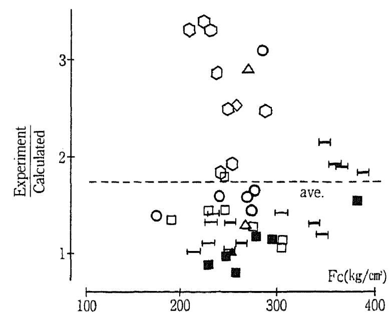

(d) Comparison of γ_3 Values at Ultimate Point

Fig.3 Comparison of Experimental Results with Calculated Results at Control Points for $\tau-\gamma$ Relationship

Table 1 Comparison of Experimental Results with Calculated Results at Control Points and Initial Stiffness for $\tau-\gamma$ Relationship

		Number of specimens	Average	Standard deviation
shear stress of 1st point (τ_1)	all specimens	57	0.98	0.21
	except①②③	51	0.98	0.18
initial stiffness (G)	all specimens	49	0.93	0.16
	except①②③	42	0.94	0.16
shear stress of 2nd point (τ_2)	all specimens	58	0.99	0.17
	except ④	51	1.00	0.17
ultimate shear stress (τ_3)	all specimens	86	1.04	0.19
	except ④	75	1.01	0.15
ultimate shear strain (γ_3)	all specimens	48	1.74	0.76
	except ④	37	1.08	0.82

N.B. ①: box wall subjected to diagonal load
②: specimen using mortar
③: PCCV
④: specimen with flexural reinforcement in flange walls

Table 2 Comparison of Experimental Results with Calculated Results at Control Points and Initial Stiffness for $M-R_B$ Relationship

		Number of specimens	Average	Standard deviation
M_1	load when flexural cracking occurs	68	0.87	0.29
	moment of 1st point for test values approximated by tri-linear curve	50	1.10	0.25
initial stiffness		41	0.93	0.35
M_2	moment of 2nd point for test values approximated by tri-linear curve	36	1.07	0.17
R_{B2}	rotational defomation of 2nd point	36	1.44	0.54
M_3	ultimate moment	18	1.09	0.15

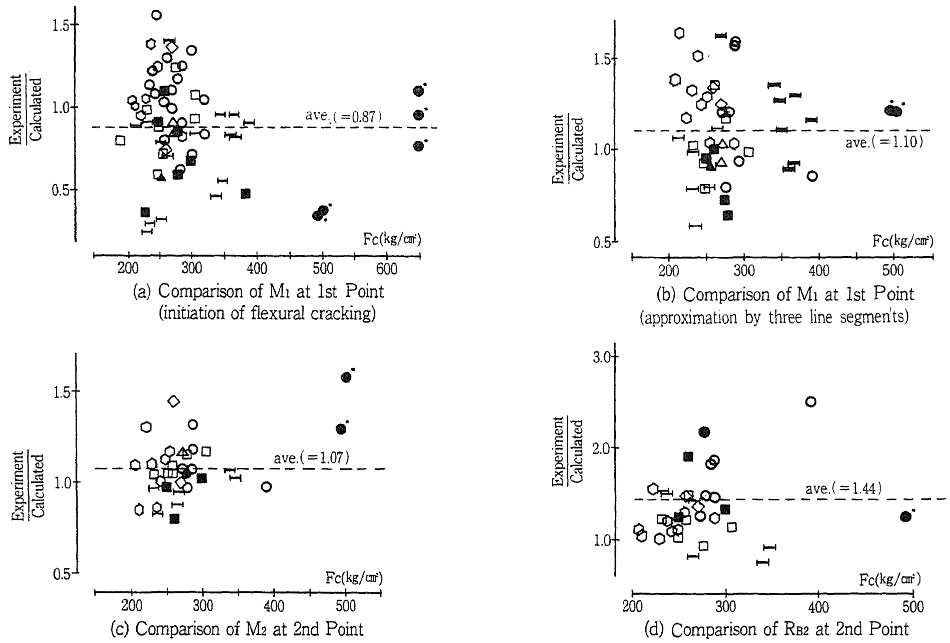

(a) Comparison of M_1 at 1st Point (initiation of flexural cracking)

(b) Comparison of M_1 at 1st Point (approximation by three line segments)

(c) Comparison of M_2 at 2nd Point

(d) Comparison of R_{B2} at 2nd Point

Fig.4 Comparison of Experimental Results with Calculated Results at Control Points for M−RB Relationship

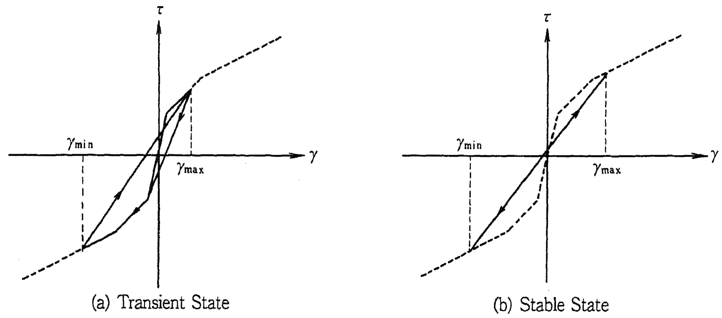

(a) Transient State

(b) Stable State

Fig. 5 Hysteresis Rules for $\tau-\gamma$ Relationship

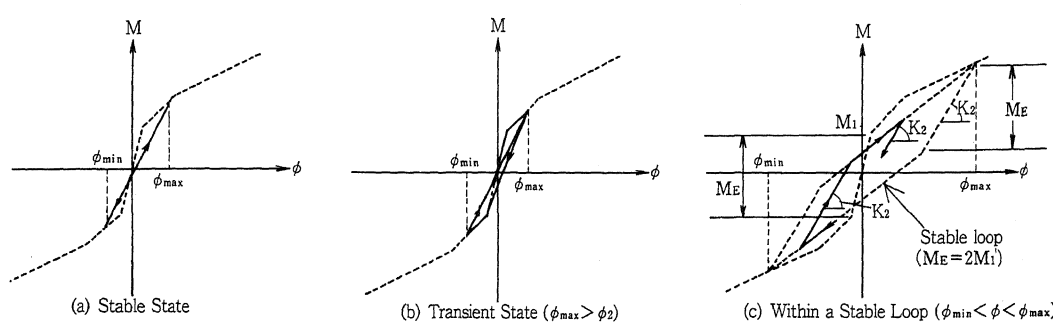

(a) Stable State

(b) Transient State ($\phi_{max} > \phi_2$)

(c) Within a Stable Loop ($\phi_{min} < \phi < \phi_{max}$)

Fig. 6 Hysteresis Rules for $M-\phi$ Relationship